Accepted Manuscript

New highly selective turn-on fluorescence receptor for the detection of copper (II)

Qian Nan, Pu Rong, Yunbao Jiang, Rui Yang

PII: S1386-1425(16)30717-X
DOI: doi: 10.1016/j.saa.2016.12.001
Reference: SAA 14814

To appear in: *Spectrochimica Acta Part A: Molecular and Biomolecular Spectroscopy*

Received date: 16 July 2016
Revised date: 3 December 2016
Accepted date: 3 December 2016

Please cite this article as: Qian Nan, Pu Rong, Yunbao Jiang, Rui Yang , New highly selective turn-on fluorescence receptor for the detection of copper (II). The address for the corresponding author was captured as affiliation for all authors. Please check if appropriate. Saa(2016), doi: 10.1016/j.saa.2016.12.001

This is a PDF file of an unedited manuscript that has been accepted for publication. As a service to our customers we are providing this early version of the manuscript. The manuscript will undergo copyediting, typesetting, and review of the resulting proof before it is published in its final form. Please note that during the production process errors may be discovered which could affect the content, and all legal disclaimers that apply to the journal pertain.

ACCEPTED MANUSCRIPT

New highly selective turn-on fluorescence receptor for the detection of copper (II)

Qian Nan[a], Pu Rong[a], Yunbao Jiang[b], *and* Rui Yang[a*]

[a] *Key Laboratory on Luminescence and Real-Time Analysis, Ministry of Education, School of Chemistry and Chemical Engineering, Southwest University, Chongqing 400715, China*

[b] *Department of Chemistry, College of Chemistry and Chemical Engineering, and the MOE Key Laboratory of Analytical Sciences, Xiamen University, Xiamen 361005, China*

[*]Corresponding author. Tel: +86 023 68367060; Fax: +86 023 68254000
E-mail address: RUIYANG@SWU.EDU.CN. (R. Yang)

[*] Corresponding author. Tel: +86 023 68367060 Fax: +86 023 68254000
E-mail address: RUIYANG@SWU.EDU.CN. (R. Yang)

ACCEPTED MANUSCRIPT

Abstract: Three new receptors (**1a–c**) bearing a *p*-dimethylaminobenzamide fluorophore have been synthesized and evaluated in terms of their fluoroionophoric properties towards various metal ions. Notably, receptors **1a** and **1c** exhibited dramatic fluorescent enhancement towards Cu^{2+} in acetonitrile. Subsequent investigations revealed that the highly selective behavior of these receptors towards Cu^{2+} could be attributed to the Cu^{2+}-mediated oxidative cyclization of these compounds to the corresponding 1,3,4-oxadiazoles. Solvent effects and quantum calculations indicated that **1a** and **1c** both possessed an intramolecular charge transfer channel, which could be obstructed by the oxidative cyclization of these receptors. Receptor **1a** was successfully applied to the determination of the Cu^{2+} in drug sample with a low detection limit of 2.2×10^{-8} mol L^{-1}.

Keywords: Fluorescence receptor; Copper (II); Oxidative cyclization; Intramolecular charge transfer

ACCEPTED MANUSCRIPT

1. Introduction

The development of new methods for the detection and monitoring of trace elements continues to attract considerable attention because of the critical roles played by these methods in biological processes. In this regard, research towards the synthesis of fluorescence receptors capable of exhibiting high levels of selectivity and sensitivity to specific metals remains an active area of interest in chemistry [1-5]. Copper is an essential trace element that is vital for maintaining the health of numerous organisms, including humans, and a large number of fluorescence receptors have been developed for the detection of Cu^{2+} in recent years [6-13]. Among those reported, receptors based on the binding [14-16] or reaction [17-19] of Cu^{2+} with a receptor, which results in pronounced changes in the spectral properties of the receptor, represent one of the main recognition mechanisms. However, Cu^{2+} is also an efficient fluorescence quenching agent because of its paramagnetic characteristics and chelating properties, which has limited the development of fluorescent receptors for the detection of Cu^{2+} [20-22]. For sensitivity reasons, receptors showing fluorescence enhancement are generally favored over those exhibiting fluorescence quenching. With this in mind, reaction-based receptors capable of overcoming the challenges posed by the paramagnetic characteristics of Cu^{2+} fold great promise for the detection of this metal. In this paper, we have developed a new strategy for the detection of Cu^{2+} based on an intramolecular charge transfer (ICT) process, which is controlled by the presence of Cu^{2+}. ICT is one of the most important characteristics of any molecule, which can be controlled by the addition of various organic donor and acceptor groups or organometallic moieties [23]. However, there have, to the best of our knowledge, been no studies reported in the literature to date concerning ICT process controlled by a metal ion-induced chemical reaction.

N-Acylhydrazones have been reported to be typical chemical reaction receptors for Cu^{2+} because they undergo an oxidative cyclization reaction in the presence of this metal ion [24]. Herein, we report the coupling of three different *N*-acyhydrazones with the ICT fluorophore *p*-dimethylaminobenzamide, to afford the corresponding benzoylhydrazones **1a–c** (Scheme 1). These receptors were synthesized with the aim of developing a deeper understanding of the influence of the ICT fluorophore on molecule characteristics of Cu^{2+} recognition. The experimental results showed that receptors **1a** and **1c** displayed high levels of selectivity towards

ACCEPTED MANUSCRIPT

Cu^{2+}, which led to large increases in the fluorescence intensities of these compounds in ACN and ACN/H_2O buffer solutions. These changes in the fluorescence properties were attributed to the Cu^{2+}-mediated oxidative cyclization of the weakly fluorescent receptor molecules to give the corresponding 1,3,4-oxadiazoles, which are rigid and highly fluorescent. These new 1,3,4-oxadiazole systems also combined with Cu^{2+} to quench the long-wavelength emissions, as well as introducing new short-wavelength emissions. We evaluated the properties of these receptors and found that they both exhibited intramolecular charge transfer (CT) characteristics, whereas no charge separation occurred in the corresponding 1,3,4-oxadiazoles. The recognition of Cu^{2+} by these receptors therefore led to a change in the CT properties of these compounds from an on state to an off state, representing a sophisticated switch for the recognition of Cu^{2+}.

Receptor **1a** was also successfully used to determine the presence of Cu^{2+} in the traditional Chinese medicine azurite, further highlighting the potential practical value of this process. Azurite contains natural copper sulfate, which can exist in a variety of different structural forms, including granular, radial and massive structures. Azurite can be used to treat various ailments, including fever, red eye pain, ear ache and lachrymatory effects and epilepsy, and is widely used as a powder or solid tablet. Notably, no methods have been reported to date for the determination of azurite.

2. Experimental

2.1. Apparatus

Fluorescence correlation spectroscopy experiments were conducted on a Hitachi F-2500 spectrofluorophotometer (Hitachi Company, Tokyo, Japan) using excitation and emission slits of 5 nm. Fluorescence quantum yields were measured using quinine sulfate as the standard (0.55 in 0.50 mol L^{-1} H_2SO_4) [25]. Absorption spectra were recorded on a UV-8500 spectrophotometer (Shimadzu Corporation, Kyoto, Japan) using a quartz cell with a path length of 1 cm. Verification tests were conducted using a TAS-986FLAA (flame atomic absorption) spectrophotometer (Persee Co.,Ltd, Beijing, China).

All of the pH measurements taken in this study were recorded on a pHS-3C pH meter (Shanghai Scientific Instruments Company, Shanghai, China). ^{1}HNMR and ^{13}CNMR spectra were recorded in DMSO-d_6 on a Varian Unity^{+} 500 MHz, Bruker AV300 and Bruker AV600 MHz spectrometer using TMS as an internal reference standard.

ACCEPTED MANUSCRIPT

The geometries of the ground and first singlet excited states were optimized under vacuum using the hybrid density functional Becke-3-Lee-Yang-Parr (B3LYP) and the single-excitation configuration interaction (CIS) method, respectively in combination with the 6-31G* basis set. All of these calculations were completed using the GAUSSIAN 2003 software package.

2.2. Reagents

p-(*N*,*N*-Dimethylamino)benzaldehyde was purchased from China National Chemicals Group (Shanghai, China). Azurite was purchased from Haocao flagship store (Bozhou, China). All of the other reagents used in this study were purchased from Sinopharm Reagent Co., Ltd (Beijing, China) and used without further purification. metal ion solutions were prepared from the corresponding perchlorate salts. Solvents for spectroscopic investigation were purified prior to being used and checked to ensure they contained no fluorescent impurities at the used excitation wavelength being used in the study. Tris-HCl buffer solutions were prepared using 0.01 mol L^{-1} Tris and the appropriate amount of HCl using a pH meter. Buffer solutions were prepared using phosphoric acid,boric acid and acetic acid to allow for the determination of the traditional Chinese medicine azurite. With the exception of acetonitrile (ACN), which was purchased as the HPLC grade, all of the chemicals used in this study were purchased as the analytical grade. Distilled water was used to prepare the aqueous solutions.

2.3. Synthesis of receptors 1a−c

The target compounds were readily synthesized using a series of simple reactions. The initial esterification of the corresponding benzoic acids with ethanol gave the ethyl benzoates, which were reacted with hydrazine hydrate to give the corresponding benzoylhydrazines. These compounds were then heated at reflux with *p*-(*N*,*N*-dimethylamino)benzaldehyde for 6 h to give the desired targets **1a–c**, as shown in Scheme 1.

(E)-N'-(4-(dimethylamino)benzylidene)benzohydrazide **(1a):** This compound was purified by repeated recrystallization from ethanol/water and characterized by ^{1}H and ^{13}C NMR spectroscopy. ^{1}H NMR (500MHz, DMSO-d_6) δ (ppm): 11.56 (s, 1H), 8.30 (s, 1H), 7.89 (d, J = 8.4 Hz, 2H), 7.51 (t, J = 7.4 Hz, 5H), 6.76 (d, J = 8.8 Hz, 2H), 2.97 (s, 6H). ^{13}C NMR (126 MHz, DMSO-d_6) δ (ppm): 162.91, 151.67, 148.89, 133.83, 131.56, 128.58, 128.51, 127.54, 121.65, 111.90, 39.83.

(E)-N'-(4-(dimethylamino)benzylidene)-2-hydroxybenzohydrazide **(1b):** This compound was purified by repeated recrystallization from *N*,*N*-dimethylformamide/water and characterized by ^{1}H

ACCEPTED MANUSCRIPT

and ^{13}C NMR. ^{1}H NMR (500 MHz, DMSO-d_6) δ (ppm):11.64 (s, 1H), 8.30 (s, 1H), 7.88 (d, *J* = 9.3 Hz, 1H), 7.57 (d, *J* = 8.9 Hz, 2H), 7.41 (s, 1H), 7.02−6.87 (m, 2H), 6.77 (d, *J* = 8.9 Hz, 2H), 2.98 (s, 6H). ^{13}C NMR (126MHz, DMSO-d_6) δ (ppm): 164.59, 159.39, 151.82, 149.91, 133.73, 128.79, 128.24, 121.29, 118.93, 117.38, 115.73, 111.87, 39.81.

(E)-N'-(4-(dimethylamino)benzylidene)-2-methoxybenzohydrazide **(1c):** This compound was purified by repeated recrystallization from ethanol/water and characterized by ^{1}H and ^{13}C NMR spectroscopy. ^{1}H NMR (600 MHz, DMSO-d_6) δ (ppm):11.16 (s, 1H), 8.18 (s, 1H), 7.62（d, *J*= 7.2 Hz, 1H）, 7.52 (d, *J*= 8.4 Hz, 2H), 7.49(t, *J*= 7.8 Hz, 1H), 7.16 (d, *J*= 8.4 Hz, 1H), 7.05 (t, *J*= 7.2 Hz, 1H), 6.76 (d, *J*= 9.0 Hz, 2H), 3.88 (s, 3H), 2.98 (s, 6H). ^{13}C NMR (75 MHz, DMSO-d_6) δ (ppm): 162.08, 157.05, 151.89, 148.37, 132.38, 130.08, 128.72, 128.10, 123.99, 121.99, 120.78, 112.21, 56.00, 39.83.

Scheme 1: Synthesis of compounds **1a−c**.

3. Results and discussion

3.1. Absorption spectrum behaviors of receptor 1a in the presence of Cu^{2+} in ACN

The absorption spectrum of receptor **1a** in ACN contained two bands at 352 and 231 nm with molar absorption coefficients of 4.28×10^4 and 1.86×10^4 M^{-1} cm^{-1}, respectively, which are indicative of the (π, π*) transition character of this compound (Fig. 1). The addition of Cu^{2+} to a solution of **1a** in ACN led to a reduction in the intensity of the band at 352 nm, as well as the appearance of two new bands (from 250 to 325 nm and 390 to 450 nm). Several other transition metal ions were also tested, including Cd^{2+}, Ni^{2+}, Zn^{2+}, Al^{3+}, Fe^{3+}, Hg^{2+} and Pb^{2+}, which all had some influence on the absorption spectrum of **1a**. In contrast, the effects of Ca^{2+}, Mg^{2+}, K^{+}, Co^{2+}, Fe^{2+}, Mn^{2+}, Cu^{+} and Ba^{2+} were negligible (Fig. S1). Based on the absorption spectra of receptor **1a** in the presence of different amounts of Cu^{2+}, we selected an isosbestic wavelength of 310 nm as the optimum excitation wavelength for all of the subsequent fluorescence measurements.

ACCEPTED MANUSCRIPT

Fig. 1 Absorption spectra of **1a** (1.5×10^{-5} mol L^{-1}) in ACN in the presence of increasing amounts of Cu^{2+} ($0.0–6.0\times10^{-5}$ mol L^{-1}).

3.2. Fluorescence spectrum behaviors of 1a in the presence of Cu^{2+} in ACN

As a solution in ACN, compound **1a** emitted weak fluorescence at 409 nm with a total fluorescence quantum yield (Φ) of 0.0079. The addition of Cu^{2+} to a solution of **1a** in ACN led to a dramatic increase in the fluorescence of **1a** (i.e., up to 160-fold). The addition of less than 1 equiv. of Cu^{2+} to a solution of **1a** in ACN led to a red-shift in the long-wavelength emission from 409 to 458 nm, as well as a sharp increase in in the fluorescence intensity (Fig. 2a). The addition of more than 1 equiv. of Cu^{2+} to a solution of 1a in ACN led to a considerable decrease in the in the intensity of the long-wavelength emission at 458 nm. This process also led to a pronounced increase in the intensity of the emission band centered at 360 nm, with an isoemissive point at 408 nm (Fig. 2b). The paramagnetic character of this metal meant that the addition of more Cu^{2+} to this solution after the fluorescence intensity at 360 nm had reached its maximum resulted in the quenching of the fluorescence emission (Fig. 2c). The unpredictable fluorescence behavior of this system in the long-wavelength emission region inspired us to investigate the recognition mechanism of this receptor in greater detail.

Fig. 2 Fluorescence spectra of **1a** (1.5×10^{-5} mol L^{-1}) in ACN in the presence of increasing amounts of Cu^{2+} (a: $0–1.5\times10^{-5}$ mol L^{-1}; b: $1.5–6.0\times10^{-5}$ mol L^{-1}; c: $6.0\times10^{-5}–4.0\times10^{-5}$ mol L^{-1}).

3.3. Solvent effects and quantum calculations

p-Dimethylaminobenzamide is a typical fluorophore with intramolecular charge transfer (ICT) characteristics. We synthesized two derivatives of *p*-dimethylaminobenzamide, compounds **1b** and **1c**, to develop a deeper understanding of the crucial role played by this moiety in receptor **1a**. The absorption and fluorescence spectra of **1a–c** were measured in several different solvents, including cyclohexane (CHX), diethyl ether (DEE), ethyl acetate (EAC) and acetonitrile (ACN), which have been arranged in order of increasing polarity. The maximum absorption peaks for compounds **1a–c** showed a continuous red-shift (Table. 1) as the polarity of the solvents increased from CHX to ACN, indicating that a ground-state charge transfer (CT) could occur [26].

ACCEPTED MANUSCRIPT

Consideration of the fluorescence spectra of receptors **1a–c** revealed that they all contained a dual fluorescence emission (Table 1 and Fig. S2), which was attributed to their *p*-dimethylaminobenzamide moiety. The short-wavelength emissions in **1a** and **1c** were found to be independent of the solvent polarity, whereas the long-wavelength emissions of these compounds showed a considerable blue-shift with increasing solvent polarity. This result was characteristic of the charge transfer properties of the excited state, and the dual fluorescence was therefore attributed to the LE and CT states [27]. The long wavelength emissions of **1b** were very weak in aprotic solvents, where the intensity as dependent on the solvent polarity. In contrast, the long wavelength emissions of this receptor showed a large blue-shift in the protic solvent methanol, most likely because this solvent prevented the formation of intramolecular hydrogen bonds between the oxygen atom of the carbonyl group and hydrogen atom of the hydroxyl group in **1b**. The lack of an intramolecular hydrogen bond would therefore inhibit the excited-state intramolecular proton transfer (ESIPT) process [28].

Table 1
The maximal absorption and emission wavelengths of **1a−c** in CHX, DEE, EAC and ACN.

To develop a deeper understanding of the emission characteristics of these receptors, we studied the geometries of the first singlet excited states of **1a** and **1c**. All calculations in this work are performed with the Gaussian 09 programs[29]. All the geometric structures of first excited stateare fully optimized using B3LYP/6-31G* method in the framework of density-functional theory (DFT)[30]. In the process of optimization, the solvent effect of CH_3CN is taken into consideration through a self-consistent reaction field (SCRF) method[31] with the polarized continuum model (PCM)[32]. The HOMO, LUMO and LUMO+1molecular orbitals of **Reactants** and **Products** are obtained in Figure 1 and 2, respectively, at the B3LYP/6-31G* calculation level (isovalue=0.02).

The results shown in Fig. 3 revealed that the HOMO orbitals of **1a** and **1c** were mainly localized on the dimethylaminobenzoyl moiety, whereas the π electrons in the LUMO orbitals were delocalized over the whole molecule. These results therefore indicated that the transition

ACCEPTED MANUSCRIPT

from HOMO to LUMO was accompanied by a charge transfer (CT) from the dimethylaminobenzoyl moiety to the whole molecule [33]. Furthermore, the quantum calculations revealed important CT channels in **1a** and **1c**.

Fig. 3 HOMO, LUMO and LUMO+1 molecular orbitals of **1a** and **1c** at the B3LYP/6-31G* calculation level (Isovalue=0.02).

3.4. Fluorescence spectrum behaviors of 1b and 1c in the presence of Cu^{2+} in ACN

The fluorescence spectra of receptors **1b** and **1c** were measured in the presence of different concentrations of Cu^{2+} to develop a deeper understanding of the effects of Cu^{2+} on the fluorescence behavior of **1a**. Receptor **1b** bearing a phenolic -OH group exhibited no fluorescent response to any of the metals examined in the current study, including Cu^{2+} in ACN. The lack of a fluorescent response in this case was attributed to the existence of an ESIPT channel in **1b**, leading to a decrease in the fluorescence quantum yield [34]. In contrast to receptor **1b**, receptor **1c** bearing a $-OCH_3$ group instead of a phenolic -OH group was found to be much more responsive to Cu^{2+}. As a solution in ACN, receptor **1c** emitted faint fluorescence with a total fluorescence quantum yield (Φ) of 0.022. This value increased up to 35-fold in the presence of Cu^{2+}, with the fluorescence spectrum of **1c** becoming increasingly similar to that of **1a**. The addition of a small amount of Cu^{2+} led to a blue-shift from 477 to 453 nm as well as a considerable increase in the emission intensity (Fig. 4a). The addition of more than 1 equiv. of Cu^{2+} resulted in a slight decrease in the intensity of the band at 453 nm, which was accompanied by a significant increase in the fluorescence intensity centered at 380 nm (Fig. 4b). After reaching its maximum value, the addition of more Cu^{2+} simply quenched the fluorescence (Fig. 4c). These results therefore indicated that receptor **1c** is highly selective for Cu^{2+} and that it most likely functions in a similar manner to **1a**.

Fig. 4 Fluorescence spectra of **1c** (1.0×10^{-5} mol L^{-1}) in ACN in the presence of increasing amounts of Cu^{2+} (a: 0–1.0×10^{-5}mol L^{-1}; b: 1.0–4.0×10^{-5}mol L^{-1}; c: 4.0×10^{-5}–3.0×10^{-4}mol L^{-1}). The excitation wavelength was 315 nm.

3.5. Recognition mechanism

Frontier molecular orbital analysis of receptors **1a** and **1c** showed that the potential binding

ACCEPTED MANUSCRIPT

sites and electron donor atoms were located on the hydrazide-hydrazine moiety. If the recognition of Cu^{2+} by these receptors was driven exclusively by an intramolecular charge transfer process induced by Cu^{2+} then the fluorescence bands in the spectra of **1a** and **1c** would both be expected to show a blue-shift in same solvent [35]. However, the fluorescence spectra of **1a** showed a red-shift after the addition of Cu^{2+} to a solution of **1a**. It is thus not possible to explain the complex changes observed in the spectra of this receptor in the presence of Cu^{2+} based on an intramolecular charge transfer mechanism alone concentrations of $KMnO_4$ (0–4.5×10^{-5} mol L^{-1}).

Fig. 5 Fluorescence spectra of **1a** (1.5×10^{-5} mol L^{-1}) in ACN in the presence of increasing amounts of $KMnO_4$ (0–4.5×10^{-5} mol L^{-1}) (red lines) and fluorescence spectra of **1a**+$KMnO_4$ solution in the presence of increasing amounts of Cu^{2+} (0–1.5×10^{-5} mol L^{-1}) (black lines).

The fluorescence emission of a receptor can not only be affected by metal ion coordination but can also be effected by metal ion-promoted reactions [36]. It has been reported that *N*-acylhydrazones can undergo an oxidative cyclization to afford 1,3,4-oxadiazoles in the presence of several oxidants, including $Cu(ClO_4)_2$ [37-39]. With this in mind, we hypothesized that Cu^{2+} would act as an oxidant prior to forming a stoichiometric ratio with **1a** (i.e., 1:1 ratio), and that this oxidant activity would result in the oxidative cyclization of **1a** to give the corresponding 1,3,4-oxadiazole. $KMnO_4$ has been widely used as an oxidant for the preparation of 1,3,4-oxadiazoles from hydrazide-hydrazones [40]. Thus, we recorded the fluorescence spectra of **1a** in ACN in the presence of several different concentrations of $KMnO_4$. A comparison of these data with those obtained for a solution of **1a** in ACN in the presence of Cu^{2+} revealed several similar spectral variations with a red-shift from 409 to 457 nm. This comparison also revealed a 30-fold increase in the fluorescence intensity following the addition of 3 equiv. of $KMnO_4$ to a solution of **1a** in ACN (Fig. 5). Compared with the Cu^{2+}, $KMnO_4$ has a low reduction speed with **1a** in ACN, thence the **1a**-$KMnO_4$ solution was placed 12 hours to obtain complete reaction. Afterwards, Cu^{2+} was added to the **1a**-$KMnO_4$ solution. As shown in Fig. 5, it was found that fluorescence at long wavelength decreased and fluorescence at short wavelength increased simultaneously, which was consistent with that of **1a** and Cu^{2+}(fig.2a and 2b). Taken together, these data demonstrate that the changes observed in the emission properties in the long-wavelength region of these spectra could be attributed to the Cu^{2+}-mediated oxidative

ACCEPTED MANUSCRIPT

cyclization of receptor **1a** to give the corresponding 1,3,4-oxadiazole.. Based on this result, we have proposed a mechanism for this process, which is shown in Scheme 2.

Scheme 2. Proposed mechanism for the response of these receptors to Cu^{2+}.

Several electrospray ionization-mass spectrometry (ESI-MS) experiments were conducted to provide experimental evidence to support this conclusion. The analysis of a solution of **1a** (10^{-4} mol L^{-1}) in ACN in the absence of Cu^{2+} by ESI-MS revealed the presence of a single mass ion with an *m/z* value of 268.1 (Fig.S3a), which was attributed to [**1a**+H]$^+$. However, the analysis of this mixture by ESI-MS following the addition of 1 equiv. of Cu^{2+} revealed the presence of three different peaks with *m/z* values of 145.0, 147.0 and 266.1 (Fig.S3b). The peaks with *m/z* values of 145.0 and 147.0 were attributed to the isotopic peaks of $[Cu(I)(CH_3CN)_2]^+$, which suggested that **1a** was being oxidized by Cu^{2+} to give Cu^+ as a reduction product [41]. In contrast, the peak with an *m/z* value of 266.1 was attributed to the 1,3,4-oxadiazole, which would have been formed by the Cu^{2+}-induced oxidative cyclization of **1a** according to the proposed kinetics process shown in Fig.S4.

The first singlet excited states of the 1,3,4-oxadiazoles resulting from the oxidative cyclization of receptors **1a** and **1c** were also studied. The results obtained following the analysis of their frontier molecular orbitals revealed that the π electrons were located across the entire molecule in both cases, and that the CT channels closed after the oxidative cyclization of receptors 1a and 1c(Fig. 6). The nitrogen and oxygen atoms in the 1,3,4-oxadiazoles could combine with Cu^{2+} to form complexes. This would explain why the addition of more Cu^{2+} to **1a** in ACN led to a gradual decrease in the fluorescence intensity of the band at 458 nm after it had reached its maximum. This would also explain the increase observed in the fluorescence emission at 360 nm (Scheme 2). The subsequent addition of a small amount of protic solvent such as methanol led to a decrease in the intensity of the short-wavelength emission at 360 nm, which was accompanied by an increase in intensity of the long-wavelength emission (Fig. S5). This change was attributed to coordination between the binding sites in the 1,3,4-oxadiazoles and Cu^{2+}, which induced the formation of a complex with the 1,3,4-oxadiazoles and Cu^{2+}. This result further illustrated that the changes observed in the long-wavelength region of the spectra resulted from the formation of the corresponding 1,3,4-oxadiazoles rather than the formation of a simple complex between Cu^{2+} and

ACCEPTED MANUSCRIPT

the receptor **1a** or **1c**.

(a) (b)

Fig. 6 HOMO, LUMO and LUMO+1 molecular orbitals of two different 1,3,4-oxadiazoles at the B3LYP/6-31G* calculation level (Isovalue=0.02).

(a) and (b) were the oxidation product of receptors **1a** and **1c**, respectively.

3.6. Selectivity

The selectivities of receptors **1a** and **1c** for Cu^{2+} were evaluated in the presence of a variety of other metal ions to investigate the effects of these ions on the fluorescence intensities of receptor **1a** and **1c**. Several metals were tested, including Zn^{2+}, Hg^{2+}, Pb^{2+}, Cd^{2+}, Ni^{2+}, Ca^{2+}, Mg^{2+}, K^{+}, Ba^{2+}, Al^{3+}, Fe^{2+}, Co^{2+}, Fe^{3+}, Cu^{+} and Mn^{2+}, which were added to ACN solutions of receptors **1a** and **1c**. The results revealed that Cu^{2+} was the only metal to have a significant effect on the fluorescence intensities of **1a** and **1c** (Fig. S6). These results also showed that the fluorescence response of **1a** to Cu^{2+} was unaffected by the presence of any other metal ion, even when the contaminating ion was present at a much higher concentration than that of Cu^{2+} (Fig. 7), indicating a good selectivity for Cu^{2+}. Notably, the response of receptor **1a** to Cu^{2+} could be readily distinguished by the naked eye under a UV lamp, as shown in Fig. S7. The high selective recognition of **1a** and **1c** towards Cu^{2+} could be attributed not only to coordination of N and O atoms, a typical example is the selective binding of amino acids to Cu^{2+}, but also to Cu^{2+} involved oxidative cyclization reaction. This is also a reason for the high sensitivity of Cu^{2+} recognition.

Fig. 7 Plot of the fluorescence enhancement (*F*) at 360 nm versus the concentrations of Cu^{2+} and several other metal ions for **1a** in ACN. Inset: the fluorescence spectra of **1a** (1.5×10^{-5} mol L^{-1}) in the presence of 1 equiv. of Cu^{2+} and 1 equiv. of Cu^{2+} plus 20 equiv. of several other metal ions.

3.7. Fluorescence spectrum behaviors of 1a in the presence of Cu^{2+} in ACN/H_2O buffer solutions

To investigate the practical application of these receptors for the detection of Cu^{2+}, we evaluated the responses of compounds **1a–c** to ACN/H_2O solutions containing Cu^{2+} ions. Receptors **1a** and **1c** showed enhanced fluorescence emission spectra following the addition of Cu^{2+} in 9:1 (v/v) mixture of ACN and H_2O, with **1a** showing a slightly higher level of

ACCEPTED MANUSCRIPT

enhancement towards Cu^{2+} than **1c** (Fig. S8). In contrast to these two receptors, **1b** had very little impact on the fluorescence emission. Based on this result, receptor **1a** was used in the subsequent experiments. We initially examined the response of receptor **1a** to a solution of Cu^{2+} in ACN/H_2O buffer solution over a range of different pH values, and pH 7.2 was found to be optimum for the quantification of Cu^{2+} using **1a** as a receptor (Fig. S9). A solution of **1a** in a 9:1 (v/v) mixture of ACN and H_2O containing Tris-HCl buffer (pH = 7.2) showed very little fluorescence emission, whereas the addition of Cu^{2+} led to a 200-fold increase in the fluorescence emission at 483 nm (Fig. 8). However, no emission bands was observed at shorter wavelengths, even after the addition of a large excess of Cu^{2+} (10 equiv.), presumably because the water molecules could prevent the complexation of the Cu^{2+} ions to the 1,3,4-oxadiazole. Several other metal ions were tested, including Zn^{2+}, Hg^{2+}, Pb^{2+}, Cd^{2+}, Ni^{2+}, Ca^{2+}, Mg^{2+}, K^{+}, Ba^{2+}, Al^{3+}, Fe^{2+}, Co^{2+}, Fe^{3+}, Cu^{+} and Mn^{2+}, but had no discernible impact on the fluorescence spectra of **1a**. This result therefore suggested that receptor **1a** could be used as a selective fluorescent receptor for the detection of Cu^{2+} in ACN/H_2O buffer solutions (Fig. S10).

The relationship between $\Delta F/F_0$ ($\Delta F = F–F_0$, where F_0 and F are the fluorescence emission intensities before and after the addition of Cu^{2+}, respectively) and the concentration of Cu^{2+} in 10^{-6} mol L^{-1} (c) was measured under the conditions described above and found to be $\Delta F/F_0 = 2.12\times10^{6}c–16.56$. The linear range of this method covered Cu^{2+} concentrations in range of 2.5×10^{-6} to 3.0×10^{-4} mol L^{-1} with a correlation coefficient of $R^2 = 0.9973$. The detection limit of this method was calculated using a previously reported procedure [38]. Briefly, the fluorescence emission spectrum of **1a** was measured 11 times and the standard deviation for the blank sample was measurement (σ). The detection limit was then calculated using the following equation: detection limit = 3σ/k, where k is the gradient of the fluorescence intensity versus the concentration of Cu^{2+}. In this case the detection limit was found to be 2.2×10^{-8}mol L^{-1}, which indicated that receptor **1a** was highly sensitive to the Cu^{2+} in the ACN/H_2O buffer solutions.

Fig. 8 Fluorescence spectra of **1a** (1.5×10^{-5} mol L^{-1}) in ACN/H_2O (9:1, *v/v*, pH=7.2)

3.8. Application of receptor 1a in azurite deterimination

Receptor **1a** was used to determine the Cu^{2+} in azurite to evaluate the practicality and efficiency of this new method. A sample solution of azurite (11.05 mg mL^{-1}) was prepared by

ACCEPTED MANUSCRIPT

dissolving powdered azurite (0.5525g) in 50mL hydrochloric acid (0.2 mol L^{-1}).

3.8.1. Procedure for evaluating the application of receptor 1a

The addition of a suitable amount of Cu^{2+} led to an increase in the intensity of the enhanced fluorescence signal. The amount of Cu^{2+} contained in a single sample of azurite can be determined theoretically using standard curves generated using a solution of **1a** as shown in Fig.9. The linear equation was ΔF= -97.72+25.53c (10^{-5} mol L^{-1}) where c is the concentration of Cu^{2+} and the correlation coefficient was 0.995.

An aliquot of the sample solution of azurite (11.05 mg mL^{-1}) prepared above was diluted 100 times with a 9:1 (v/v) mixture of ACN and water. The pH of the diluted sample solution was 3.00, so buffer solution (pH = 3.12) was selected to replace the water in the mixture. The buffer solution was prepared with phosphoric acid, boric acid and acetic acid. Notably, the H^+ ions present in the mixture could cause fluorescence quenching and the presence of other ions could interfere with the results, which may explain the poor linearity of this plot.

Fig. 9 Linear plot of ΔF versus the concentration of Cu^{2+} for the reaction of Cu^{2+} with **1a**

3.8.2. Recovery and accuracy properties

The accuracy and precision characteristics of our newly developed method were determined by the repeated analysis of samples containing five different concentrations of Cu^{2+}. The recovery values were determined to be in the range of 97.9–102.4 ± 1.02–2.16% (Table 2), thereby highlighting the accuracy of our new method for the determination of Cu^{2+}. Consideration of the results obtained for the different concentrations revealed that the average recovery was 99.78±1.71%, demonstrating the good accuracy and reproducibility of this method.

Table 2

Recovery studies for the determination of azuritum based on its reaction with FLP according to our new method.

3.8.3. Trial experiment

The experiment results were examined using the standard addition method by atomic adsorption spectrometry (AAS), and the results are shown in Tables 3 and 4. Figures. S11 and S12 show the linear graphs obtained from the AAS experiments , the correlation coefficient were 0.99966 and

ACCEPTED MANUSCRIPT

0.99983. The actual Cu^{2+} contents of the test samples of azurite were determined to be 24.48 and 22.51%, respectively, representing an average Cu^{2+} content of 23.50%. The sample solution (11.05 mg mL^{-1}) was then diluted 100 times with a 9:1 (v/v) mixture of ACN and water. A 500 μL aliquot of this diluted material was then transferred to a cuvette containing 1800 mL of ACN and 200 mL of buffer solution, and the final percentage mass content was 23.60%. This result was close to the value of 23.50% obtained by AAS. Taken together, these data show that our newly developed fluorometric method is highly sensitive with a low detection limit and good accuracy.

Table 3

Results for the detection of Cu^{2+} in azurite using the standard addition method by AAS

Table 4

Results for detection of Cu^{2+} in azurite using the standard addition method by AAS

4. Conclusion

We have designed and synthesized two simple, neutral receptors (**1a** and **1c**), which showed high levels of selectivity towards Cu^{2+} in ACN and ACN/H_2O buffer solutions. Notably, receptor **1a** was successfully applied to the detection of Cu^{2+} in practical samples with satisfied recovery and accuracy characteristics. Although receptor**s 1a** and **1c** exhibited intramolecular charge transfer (ICT) characteristics, they also showed dramatic fluorescence enhancement in response to Cu^{2+}. This enhancement effect was attributed to the Cu^{2+}-mediated oxidative cyclization of the non-fluorescent receptors to give the corresponding 1,3,4-oxadiazoles, which are rigid and highly fluorescent. Furthermore, the ICT channels of these receptors were closed after they underwent the oxidative cyclization process. We have therefore developed a new strategy for the construction of fluorescent receptors.

Acknowledgments

This work was supported by the National Natural Science Foundation of China (Grant no. 20835005) and the Doctoral Foundation of Southwest University (SWUB2008044).

ACCEPTED MANUSCRIPT

References

[1] S. Goswami, D. Sen, N.K. Das, Org. Lett. 12 (2010) 856-859.

[2] Z.X. Li, L.F. Zhang, L.N. Wang, Y.K. Guo, L.H. Cai, M.M. Yu, L.H. Wei, Chem. Commun, 47 (2011) 5798-5800.

[3] H.H. Wang, L. Xue, Z.J. Fang, G.P. Li, H. Jiang, New J. Chem. 34 (2010) 1239-1242.

[4] Z.J. Zhou, N. Li, A.J. Tong, Anal. Chim. Acta, 702 (2011) 81-89.

[5] Y.Y. Ma, H. Liu, S.P. Liu, R. Yang, Analyst. 137 (2012) 2313-2317.

[6] C.W. Yu, L.X. Chen, J. Zhang, J.H. Li, P. Liu, W.H. Wang, B. Yan, Talanta. 3 (2011) 1627-1633.

[7] Y. Zhou, F. Wang, Y. Kim, S.J. Kim, J. Yoon, Org. Lett. 11 (2009) 4442-4445.

[8] L. Huang, J. Cheng, K.F. Xie, P.X. Xi, F.P. Hou, Z.P. Li, G.Q. Xie, Y.J. Shi, H.Y. Liu, D.C. Bai, Z.Z. Zeng, Dalton. Trans. 40 (2011) 10815-10817.

[9] V. Dujols, F. Ford, A.W. Czarnik, J. Am. Chem. Soc. 119 (1997) 7386-7387.

[10] X. Zhang, Y. Shiraishi, T. Hirai, Org. Lett. 9 (2007) 5039-5042.

[11] Z.C. Wen, R. Yang, H. He, Y.B. Jiang, Chem. Commun. 1 (2006) 106-108.

[12] C.W. Yu, J. Zhang, J.H. Li, P. Liu, P.H. Wei, L.X. Chen, Microchim Acta. 174 (2011) 247-255.

[13] L. Jiao, J. Li, S. Zhang, C. Wei, E. Hao, M.G.H. Vicente, New J. Chem. 33 (2009) 1888-1893.

[14] Z. Li, E.W. Miller, A. Pralle, E.Y. Isacoff, C.J. Chang, J. Am. Chem. Soc. 128 (2006) 10-11.

[15] Z.C. Xu, Y. Xiao, X.H. Qian, J.N. Cui, D.W. Cui, Org. Lett. 7 (2005) 889-892.

[16] R. Joseph, J.P. Chinta, C.P. Rao, Inorg. Chim. Acta. 12 (2010) 2833-2839.

[17] N. Li, Y. Xiang, A.G. Tong, Chem. Commun. 46 (2010) 3363-3365.

[18] M.H. Kim, H.H. Jang, S. Yi, S.K. Chang, M.S. Han, Chem. Commun. 32 (2009) 4838-4840.

[19] M. Kumar, N. Kumar, V. Bhalla, P.R. Sharma, T. Kaur, Org. Lett. 14 (2012) 406-409.

[20] Z.T. Jiang, R.R. Deng, L. Tang, P. Lu, Sens. Actuators, B. 135 (2008) 128-132.

[21] H.H. Wang, L. Xue, Z.J. Fang, G.P. Li, H. Jiang, New J. Chem. 34 (2010) 1239-1242.

[22] Y.Q. Weng, F. Yue, Y.R. Zhong, B.H. Ye, Inorg. Chem. 46 (2007) 7749-7755.

[23] L.O. Pålsson, C.S. Wang, A.S. Batsanov, S.M. King, A. Beeby, A.P. Monkman, and M.R. Bryce, Chem. Eur. J. 16 (2010) 1470-1479.

[24] A.F. Li, H. He, Y.B. Ruan, Z.C. Wen, J.S. Zhao, Q.J. Jiang, Y.B. Jiang, Org. Biomol. Chem. 7

ACCEPTED MANUSCRIPT

(2009) 193-200.

[25] J.N. Demas, G.A. Crobys, J. Phys. Chem. 75 (1971) 991-1024.

[26] J. Herbich, A. Kapturkiewicz, J. Am. Chem. Soc. 120 (1998) 1014-1029.

[27] D. Braun, W. Rettig, S. Delmond, J.F. Le´tard, R. Lapouyade, J. Phys. Chem. A. 101 (1997) 6836-6841.

[28] J. Seo, S. Kim, S.Y. Park, J. Am. Chem. Soc. 126 (2004) 1154-1155.

[29] M.J. Frisch, G.W. Trucks, H.B. Schlegel, G.E. Scuseria, M.A. Robb, J.R. Cheeseman, G. Scalmani, V. Barone, B. Mennucci, G.A. Petersson, H. Nakatsuji, M. Caricato, X. Li, H.P. Hratchian, A.F. Izmaylov, J. Bloino, G. Zheng, J.L. Sonnenberg, M. Hada, M. Ehara, K. Toyota, R. Fukuda, J. Hasegawa, M. Ishida, T. Nakajima, Y. Honda, O. Kitao, H. Nakai, T. Vreven, J.A. Jr.Montgomery, J.E. Peralta, F. Ogliaro, M. Bearpark, J.J. Heyd, E. Brothers, K. N. Kudin, V.N. Staroverov, R. Kobayashi, J. Normand, K. Raghavachari, A. Rendell, J.C. Burant, S.S. Iyengar, J. Tomasi, M. Cossi, N. Rega, J.M. Millam, M. Klene, J.E. Knox, J. B. Cross, V. Bakken, C. Adamo, J. Jaramillo, R. Gomperts, R.E. Stratmann, O. Yazyev, A.J. Austin, R. Cammi, C. Pomelli, J.W. Ochterski, R.L. Martin, K. Morokuma, V.G. Zakrzewski, G.A. Voth, P. Salvador, J.J. Dannenberg, S. Dapprich, A.D. Daniels, O. Farkas, J.B. Foresman, J.V. Ortiz, J. Cioslowski, D.J. Fox, Gaussian 09, Revision A.02; Gaussian, Inc.: Wallingford, CT, 2009.

[30] R.G. Parr, R.G.P.W. Yang, Oxford university press. 3 (1980) 5-15.

[31] (a) G. Rauhut, T. Clark, T. Steinke, J. Am. Chem. Soc. 115 (1993) 9174-9181.

(b) M.W. Wong, K.B. Wiberg, M.J. Frisch, J. Am. Chem. Soc. 114 (1992) 1645-1652.

[32] (a) S. Miertus, J. Tomasi, Chem. Phys. 65 (1982) 239-245.

(b) M. Cossi, G. Scalmani, N. Rega, V. Barone, J. Chem. Phys. 117 (2002) 43-54.

(c) T. Mineva, N. Russo, E. Sicilia, J. Comput. Chem. 19 (1998) 290-299.

[33] E. Bardez, I. Devol, B. Larrey, B. Valeur, J. Phys. Chem. B. 101 (1997) 7786-7793.

[34] X. Zhang, C.J. Wang, L.H. Liu, Y.B. Jiang, J. Phys. Chem. B. 106 (2002) 12432-12440.

[35] P. Dumon, G. Jonusauskas, F. Dupuy, P. Pe´e, C. Rullibe´re, J. Phys. Chem. 98 (1994) 10391-10396.

[36] Y. Xiang, A.G. Tong, Luminescence. 23 (2008) 28-31.

[37] T. Chiba, M. Okimoto, J. Org. Chem. 57 (1992) 1375-1379.

ACCEPTED MANUSCRIPT

[38] S. Rostamizadeh, S.A.G. Housaini, Tetrahedron Lett. 45 (2004) 8753-8756.

[39] S. Buscemi, M. Gruttadauria, Tetrahedron. 56 (2000) 999-1004.

[40] S.H. Mashraqui, S. Sundaram, A.C. Bhasikuttan, Tetrahedron. 63 (2007) 1680-1688.

[41] Y. Xiang, A.J. Tong, Luminescence 23 (2008) 28-31.

ACCEPTED MANUSCRIPT

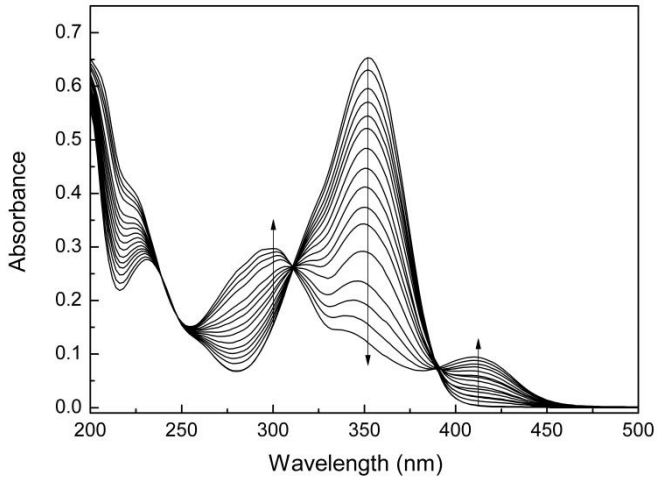

Fig. 1 Absorption spectra of **1a** (1.5×10^{-5} mol L^{-1}) in ACN in the presence of increasing amount of Cu^{2+} ($0.0–6.0\times10^{-5}$ mol L^{-1}).

ACCEPTED MANUSCRIPT

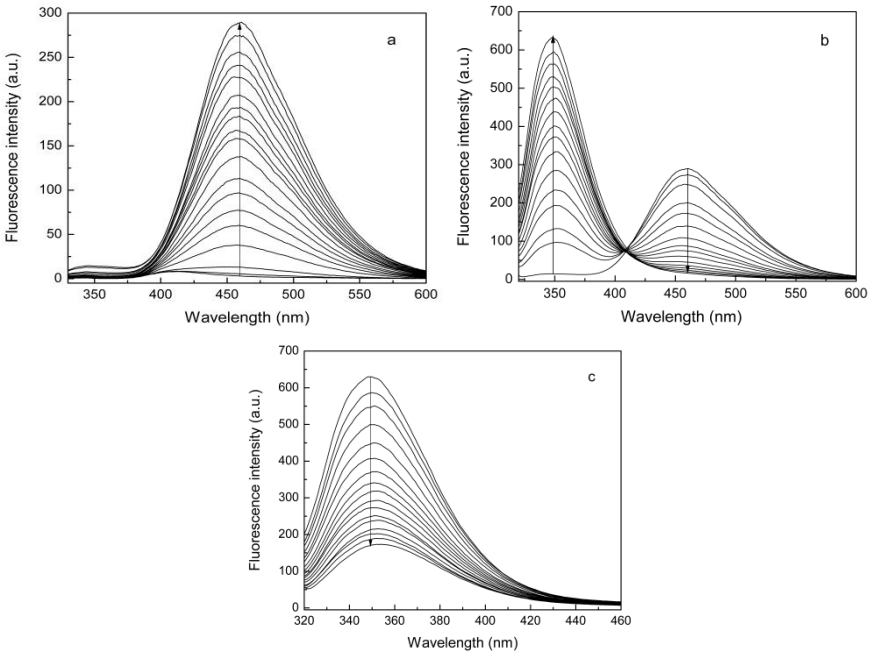

Fig. 2 Fluorescence spectra of **1a** (1.5×10^{-5} mol L^{-1}) in ACN in the presence of increasing amounts of Cu^{2+} (a: 0–1.5×10^{-5} mol L^{-1}; b: 1.5–6.0×10^{-5} mol L^{-1}; c: 6.0×10^{-5}–4.0×10^{-5} mol L^{-1}).

ACCEPTED MANUSCRIPT

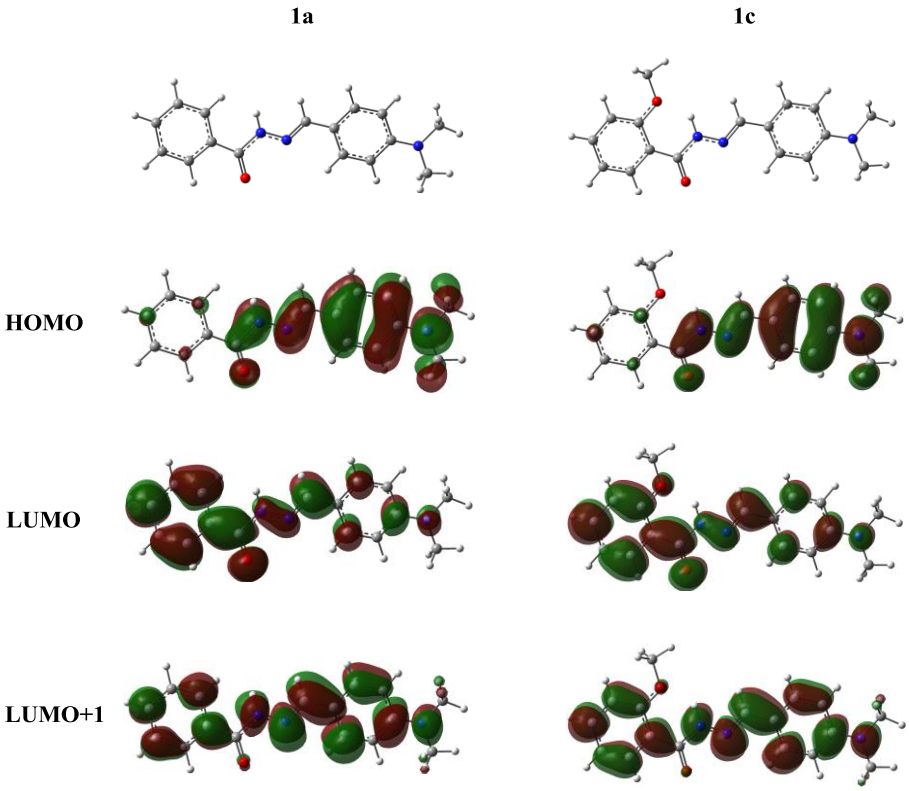

Figure. 3 HOMO, LUMO and LUMO+1 molecular orbitals of **1a** and **1c** at the B3LYP/6-31G* calculation level (Isovalue=0.02).

ACCEPTED MANUSCRIPT

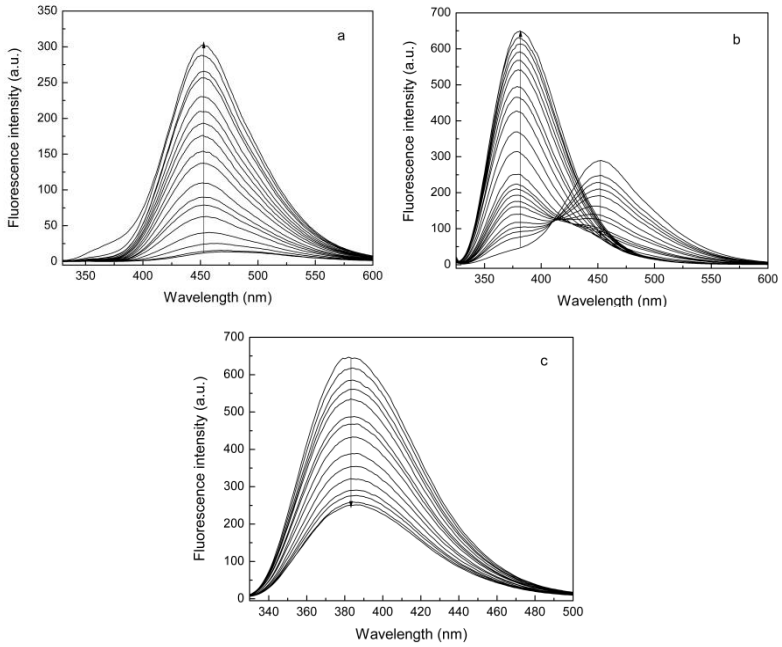

Fig. 4 Fluorescence spectra of **1c** (1.0×10^{-5} mol L^{-1}) in ACN in the presence of increasing amounts of Cu^{2+} (a: 0–1.0×10^{-5}mol L^{-1}; b: 1.0–4.0×10^{-5}mol L^{-1}; c: 4.0×10^{-5}–3.0×10^{-4}mol L^{-1}). The excitation wavelength was 315 nm.

ACCEPTED MANUSCRIPT

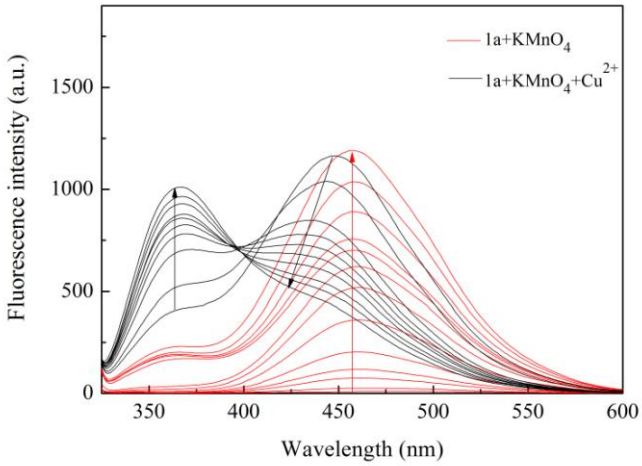

Fig. 5 Fluorescence spectra of **1a** (1.5×10^{-5} mol L^{-1}) in ACN in the presence of increasing amounts of $KMnO_4$ (0–4.5×10^{-5} mol L^{-1}) (red lines) and fluorescence spectra of **1a**+$KMnO_4$ solution in the presence of increasing amounts of Cu^{2+} (0–1.5×10^{-5} mol L^{-1}) (black lines).

ACCEPTED MANUSCRIPT

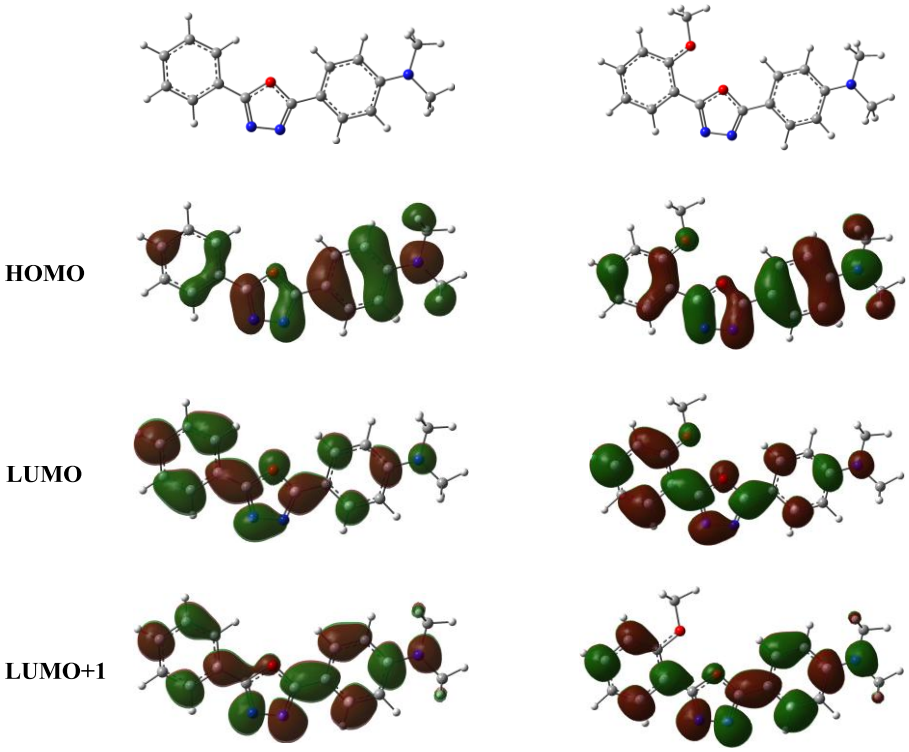

(a) (b)

Fig. 6 HOMO, LUMO and LUMO+1 molecular orbitals of two different1,3,4-oxadiazoles at the B3LYP/6-31G* calculation level (Isovalue=0.02).

(a) and (b) were the oxidation product of receptors **1a** and **1c**, receptively.

ACCEPTED MANUSCRIPT

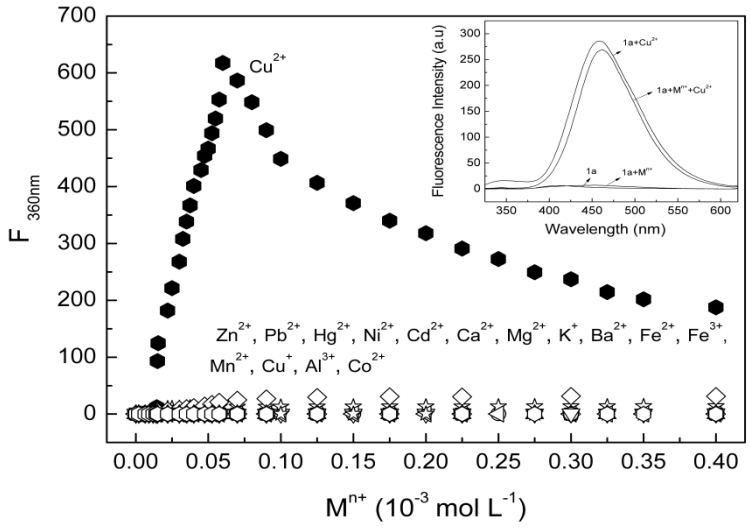

Fig. 7 Plot of the fluorescence enhancement (*F*) at 360 nm versus the concentrations of Cu^{2+} and several other metal ions for **1a** in ACN. Inset: the fluorescence spectra of **1a** (1.5×10^{-5} mol L^{-1}) in the presence of 1 equiv. of Cu^{2+} and 1 equiv. of Cu^{2+} plus 20 equiv. of several other metal ions.

ACCEPTED MANUSCRIPT

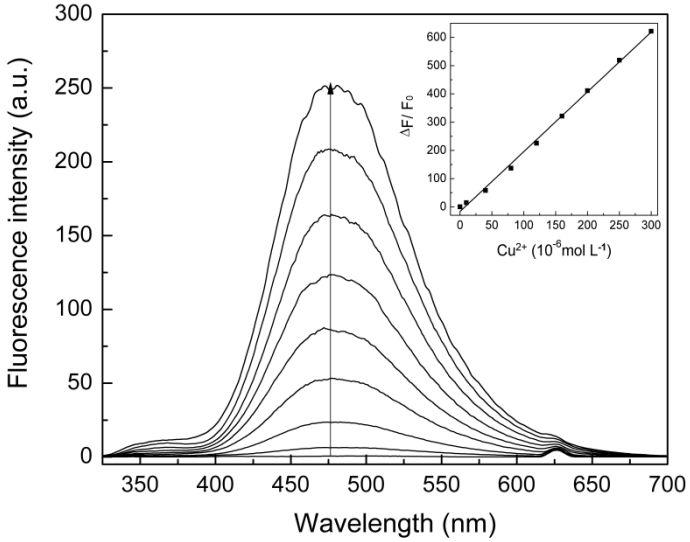

Fig. 8 Fluorescence spectra of **1a** (1.5×10^{-5} mol L^{-1}) in ACN/H_2O (9:1, *v/v*, pH=7.2)

ACCEPTED MANUSCRIPT

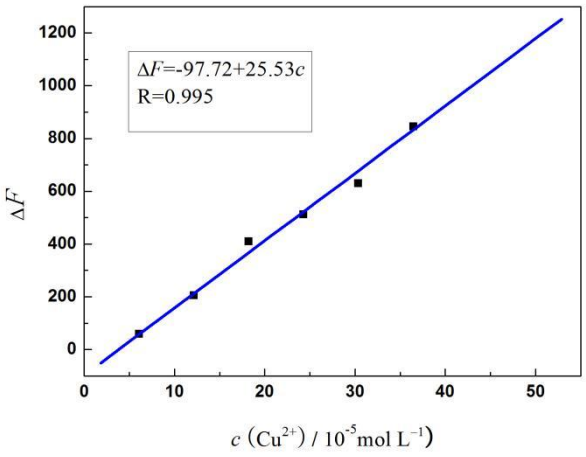

Fig. 9 Linear plot of ΔF versus the concentration of Cu^{2+} for the reaction of Cu^{2+} with **1a**

ACCEPTED MANUSCRIPT

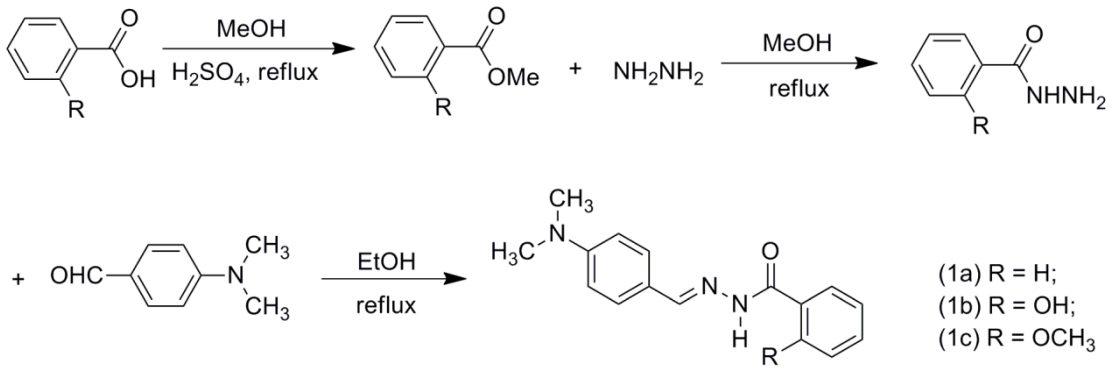

Scheme 1: Synthesis of compounds **1a−c**.

ACCEPTED MANUSCRIPT

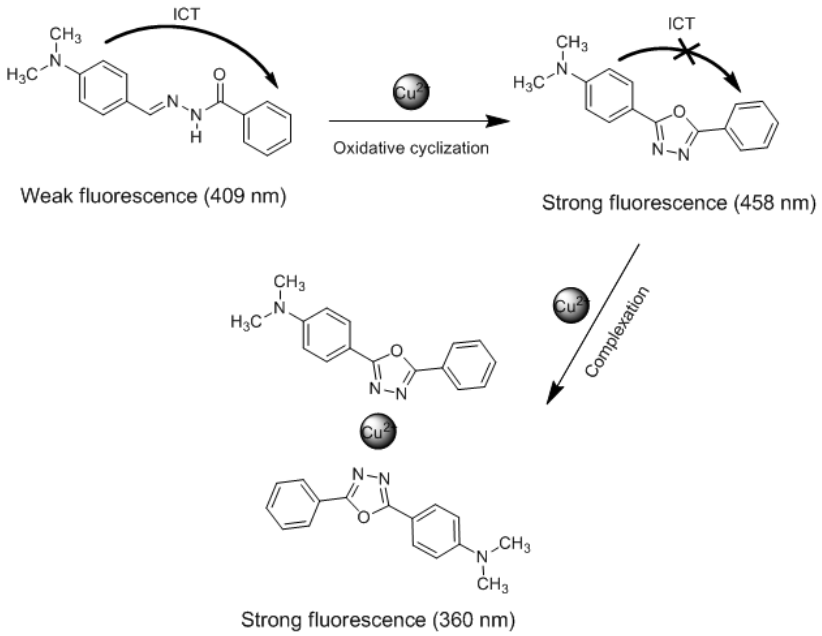

Scheme 2. Proposed mechanism for the response of these receptors to Cu^{2+}.

ACCEPTED MANUSCRIPT

Table1

The maximal absorption and emission wavelengths of **1a−c** in CHX, DEE, EAC and ACN.

	1a		**1b**		**1c**	
Solvent	λ_{Ab}	$\lambda_{LE}/\lambda_{CT}$	λ_{Ab}	$\lambda_{LE}/\lambda_{PT}$	λ_{Ab}	$\lambda_{LE}/\lambda_{CT}$
CHX	342	343/395	377	377/423	348	349/393
DEE	344	343/397	378	377/423	349	348/404
EAC	347	343/407	381	377/423	350	349/416
ACN	353	343/409	388	377/425	357	349/477

ACCEPTED MANUSCRIPT

Table 2

Recovery studies for the determination of azuritum based on its reaction with FLP according to our new method.

Taken(μg mL^{-1})	recovery(%±SD)*
5.52	102.4±1.02
22.1	98.7±2.03
44.2	97.9±2.16
66.3	100.1±1.78
110.5	99.8±1.57
Average	99.78±1.71

ACCEPTED MANUSCRIPT

Table 3

Results for the detection of Cu^{2+} in azurite using the standard addition method by AAS

Number	Measuring object	Abs	concentration [µg mL^{-1}]	Actual content [µg g^{-1}]	Weight [g]	Volume [mL]
1	blank sample	0.002				
2	standard sample	0.107	0.00			
3	standard sample	0.219	0.50			
4	standard sample	0.322	1.00			
5	standard sample	0.424	1.50			
6	standard sample	0.521	2.00			
7	sample		0.541	244826.3	0.5525	250000

ACCEPTED MANUSCRIPT

Table 4

Results for detection of Cu^{2+} in azurite using the standard addition method by AAS

Number	Measuring object	Abs	concentration [μg mL^{-1}]	Actual content [μg g^{-1}]	Weight [g]	Volume [mL]
1	blank sample	0.002				
2	standard sample	0.098	0.00			
3	standard sample	0.200	0.50			
4	standard sample	0.306	1.00			
5	standard sample	0.400	1.50			
6	standard sample	0.500	2.00			
7	sample		0.497	225106.4	0.5525	250000

ACCEPTED MANUSCRIPT

Graphical abstract

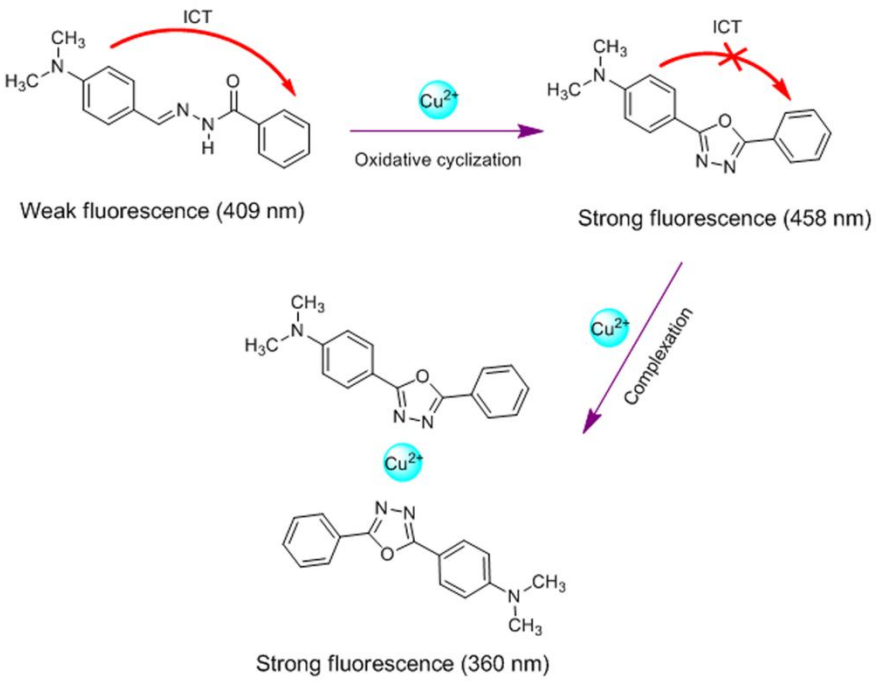

ACCEPTED MANUSCRIPT

Highlights

►Three new “turn-on” type Cu^{2+} fluorescence receptors have been synthesized.

►This mechanism involved the Cu^{2+}-mediated oxidative cyclization of the receptor.

►Charge transfer from an “on” to “off” state following the recognition of Cu^{2+}.

►This receptor was successfully used to determine Cu^{2+} in practical samples.